Structural characterization and high throughput screening of inhibitors of PvdQ, an NTN hydrolase involved in pyoverdine synthesis.

Eric J. Drake and Andrew M. Gulick

Supplemental Material

***Ab Initio Phasing and Structure determination of PvdQ*.**

Coincident with our determination of the structure of PvdQ by MAD phasing methods, the structure was also determined by Molecular Replacement (*1*). Although grown from different conditions, our crystals were isomorphous with the crystals grown by Bokhave et al. The final structural models are highly similar to the prior structures, however the exact fatty acyl component differs between our structures presented here and the recently published structures. The structures bound to specific inhibitors of PvdQ are presented in the main text. This supplemental material presents the structure determination by experimental phasing for PvdQ bound to a copurified fatty acid, modeled as octanoate, and acylated with myristate on the active site serine residue.

PvdQ crystals were optimized from leads first identified in the 1536 microbatch crystallization screen provided by the Center for High Throughput Structural Biology at the Hauptman-Woodward Institute (*2*). Crystals of the native protein were grown at 20°C by hanging drop vapor diffusion using a 1:1 mixture of protein and precipitant containing 10-15% PEG 4000, 50-100 mM RbCl, and 50 mM Hepes (pH 7.5). Native crystals were mounted in nylon loops and cryoprotected by transferring through five solutions containing increasing amounts of ethylene glycol (8%, 12%, 16%, 20%, 24%) for approximately 20 seconds each and stored in liquid nitrogen. The final cryoprotectant solution contained 24% ethylene glycol, 15% PEG 4000, 0.1 M RbCl, and 50 mM Hepes (pH 7.5). SeMet crystals were optimized to 17-22% PEG 4000, 80-100 mM RbCl, and 50 mM Hepes (pH 7.5). For substrate soaks the crystals were placed in the first cryo solution with 2mM *p*-nitrophenyl myristate for 15 minutes. They were then transferred through the remaining cryo solutions that contained appropriate substrate concentrations.

A 2.1Å three-wavelength MAD dataset was collected remotely at the Stanford Synchrotron Radiation Laboratory using a SeMet labeled crystal. The heavy atom substructure was

determined with SOLVE (*3*) and refined by solvent flattening with RESOLVE (*4*). Automated chain tracing with RESOLVE resulted in the placement of 635 residues, 478 of which were placed within the sequence. The phases from RESOLVE were merged with a higher resolution dataset derived from a crystal that was soaked with *p*-nitrophenyl myristate. This partially phased dataset was then submitted to ARP/wARP for automated tracing. The resulting model was used for continued cycles of manual model building with COOT (*5*) and refinement with REFMAC5 (*6*). Clear difference density was observed for the myristate chain that was continuous with the $O\gamma$ of Ser217. An acyl linkage between the myristate and Ser217 was modeled into this density. Refinement resulted in a small degree of difference density in the area of the linkage suggesting that free fatty acid is present at low occupancy. TLS anisotropic B-factor refinement was included in the final stages of refinement for the protein chains. The TLS server (*7*) was used to identify six segments for TLS group definition.

Subsequently, a dataset of a presumed native crystal was collected. This structure was solved by difference Fourier methods using the nearly complete structure of the acylated model, from which waters and heteroatoms were removed. As the structure was refined, it became clear that the acyl binding pocket contained density that could be fit by a medium chain fatty acid. As no ligands were added to this protein crystal, we believe that the fatty acid was co-purified with the protein. The coordinates for an octanoate molecule were included in the final model at full occupancy; based on density and B-factor analysis, it is likely to be present at less than full occupancy. Evidence for radiation damage was apparent in the model of the octanoate bound structure, including several decarboxylated glutamate residues and evidence for partial breakage of the three disulfide bonds. Again, at final stages, TLS refinement was included.

Table S1. Crystallographic Data

	SeMet PvdQ Peak	SeMet PvdQ Inf	SeMet PvdQ Rem	PvdQ + Octanoate	Acylated PvdQ
Data Collection					
Beamline	SSRL 11-1	SSRL 11-1	SSRL 11-1	CHESS A1	SSRL 9-2
PDB Code				**3L91**	**3L94**
Wavelength (Å)	0.97837	0.97887	0.9558	0.9782	0.9795
Resolution (Å)	50.0 - 2.1	50.0 - 2.1	50.0 - 2.1	30.0 - 1.65	30.0 - 1.95
Space Group	$C222_1$			$C222_1$	$C222_1$
Unit Cell (Å)	a=120.4			a=120.3	a=120.4
	b=165.6			b=165.3	b=165.6
	c=93.7			c=94.0	c=93.7
R_{merge}[a](%)	6.2	6.0	5.7	4.5	8.7
	(14.2)	(14.6)	(16.2)	(35.4)	(49.7)
Completeness[a] (%)	99.5	99.4	99.7	93.8	100.0
	(98.9)	(97.0)	(99.3)	(62.9)	(99.6)
I/σ[a]	23.4	23.0	21.1	19.0	13.3
				(2.1)	(2.3)
# Observations	228769	228933	230466	361223	277559
# Reflections	54887	54846	55006	103682	68791
Refinement					
Refinement Resolution (Å)				30.0 - 1.66	30.0 - 1.95
R-factor[a](%)				16.8 (28.1)	17.3 (24.6)
R-free[a](%)				18.5 (28.8)	20.0 (28.4)
Wilson B-value($Å^2$)				22.7	20.8
Average B-Factor, Overall[b]($Å^2$)				24.3, 23.5, 25.1	25.3, 24.5, 26.2
Average B-Factor, Solvent($Å^2$)				26.0	29.0
Average B-Factor, ligands[c]($Å^2$)				41.2, 44.2	33.3, 30.2
RMS Deviation, Bond Lengths, Angles(Å, °)				0.011, 1.23°	0.014, 1.34°

[a]Values in parentheses are for the highest resolution shell.
[b]Values are presented for all protein atoms, backbone, and side chain atoms, respectively
[b]Values are presented for ethylene glycol and fatty acid atoms, respectively

Electron Density of Crystals Soaked with Acyl-Pyoverdine precursor.

We soaked native crystals with the acyl-pyoverdine precursor PVDIq to attempt to obtain a structure of the protein bound to either the true substrate or the acyl-enzyme intermediate. As noted, the "native" protein crystals that were not soaked with a ligand showed electron density interpreted as a molecule of octanoate bound non-covalently in the fatty acid binding pocket. We incubated these crystals, derived from a single experimental plate, through a series of lower pH solutions and subsequently for multiple time points at pH 5 with the acyl-pyoverdine precursor obtained from the *pvdQ* deletion strain of cells. At 10 minutes, the active site showed no evidence of a fatty acid present in the active site (Figure S1A). The structure resulting from a 2 h soak contained a covalently bound myristate molecule (Figure S1B), a result that was consistent with our identification of the chemical nature of the acyl chain incorporated by the adenylation domain of PvdL module 1. To convincingly demonstrate that the co-purified octanoate molecule was successfully removed from the active site, and to demonstrate the covalent linkage observed with the 2h soak with the acyl-pyoverdine molecule, we present here the electron density of the initial, unrefined molecular models that result from the initial molecular replacement and a single round of refinement with REFMAC.

The maps clearly show the difference between the 10 min soak or the 2 h soak. 2*F*o-*F*c density (purple and blue) is contoured at 1σ and *F*o-*F*c density is contoured at +3σ (green) and –3σ. (red) The positive Fo-Fc density in the 10 min soak near the serine hydroxyl is from a solvent molecule.

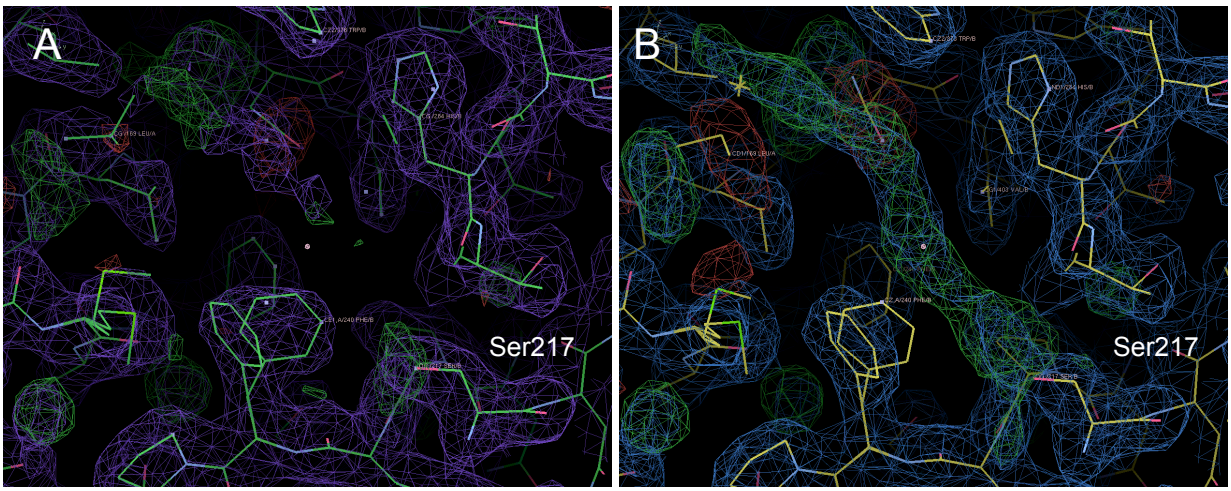

Figure S1. Electron density of initial molecular model of crystal soaked for A. 10 min and B. 2 h with acyl-pyoverdine precursor PVDIq. Residue Serβ217 is labeled in both figures. Phe240 and Met246 are present in multiple side chain torsion angles derived from the search model used for molecular replacement.

Mass Spectrometry Analysis of Pyoverdine Isoforms

The pyoverdine molecule expressed from *P. aeruginosa* PA01 is a population of isoforms. At least seven different peaks have been reported (*8*) that include variations in the saturation of the central ring of the chromophore (forming dihydropyoverdine), differences in the amino terminal "side arm", which has been reported to be succinate, succinamide, malate, and glutamate. The material obtained via HPLC separation of pyoverdine peaks was subjected to MALDI-TOF mass spectrometry to confirm the acylation state of the pyoverdines isolated. We present here plausible structures of the three highest peaks from our analysis (Table S2 and Figure S1).

Table S2

Peak (m/z)	Rel Intensity	Explanation	Calculated
Pyoverdine isolated from media from wild-type *P. aeruginosa* PA01			
1333.4	1.0	Mature pyoverdine (**S1**)	1333.61
1315.3	0.5	Dehydration of **S1** at Ser or Thr residue	1315.60
1335.4	0.2	Dihydropyoverdine (**S2**)	1335.63
Pyoverdine isolated from media from *pvdQ* deletion strain			
1559.4	1.0	Myristoyl-Pyoverdine (**S3**, PvdIq)	1559.81
1561.4	0.9	Myristoyl-Dihydrochromophore (**S4**)	1561.82
1533.3	0.2	Loss of formate from N-formyl-N-hydroxyornithine	1533.83
Pyoverdine isolated from media from *pvdQ* strain incubated with PvdQ enzyme			
1321.3	1.0	Deacylation and loss of formyl group (**S5**)	1321.61
1351.4	0.8	Deacylation of dihydrochromophore (**S6**)	1351.62
1307.2	0.3	Decarboxylation of aspartyl group	1307.63

Three samples were analyzed by MS. We first isolated pyoverdine from media of wild-type PA01. The most prominent peak was confirmed to be mature pyoverdine **S1**, with a succinamide side arm and a double bond in the central ring of the chromophore. Also identified were dihydropyoverdine (**S2**) and a dehydration product, likely at one of the serine or threonine side chains. We then isolated the pyoverdine from the media of a *pvdQ* deletion strain. While less material was obtained, it was possible to separate the peaks and detect via MS. The same batch of isolated media was split in two; one half of the sample was incubated with purified

PvdQ for one hour at 37°C, while the remaining sample was incubated with buffer alone. The buffer-treated sample demonstrated larger m/z, showing the presence of the myristoyl group. The two major peaks were acyl-Pvd containing the single (**S3**) and double (**S4**) bond character of the central ring. In contrast, the pyoverdine sample that was treated with PvdQ that co-migrated with mature pyoverdine from wild-type cells showed m/z values that demonstrated the loss of the myristoyl chain (**S5** and **S6**).

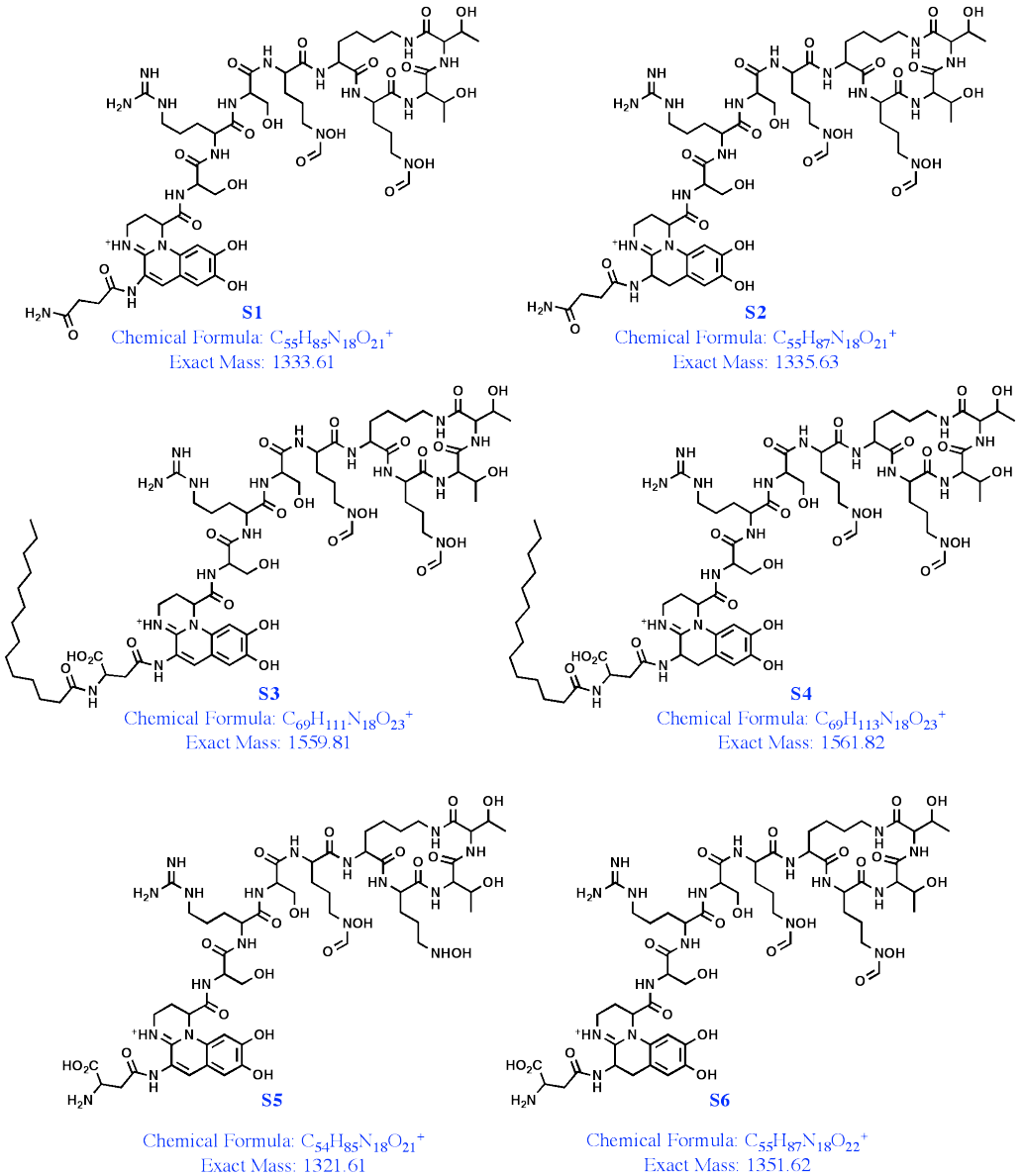

Figure S2. Chemical structures of pyoverdine isoforms characterized by mass spectrometry following separation with HPLC.

Supplemental References

1. Bokhove, M., Jimenez, P. N., Quax, W. J., and Dijkstra, B. W. (2010) The quorum-quenching N-acyl homoserine lactone acylase PvdQ is an Ntn-hydrolase with an unusual substrate-binding pocket, *Proc Natl Acad Sci U S A 107*, 686-691.
2. Luft, J. R., Collins, R. J., Fehrman, N. A., Lauricella, A. M., Veatch, C. K., and DeTitta, G. T. (2003) A deliberate approach to screening for initial crystallization conditions of biological macromolecules, *J Struct Biol 142*, 170-179.
3. Terwilliger, T. C., and Berendzen, J. (1999) Automated MAD and MIR structure solution, *Acta Crystallogr D Biol Crystallogr 55*, 849-861.
4. Terwilliger, T. C. (2001) Maximum-likelihood density modification with pattern recognition of structural motifs, *Acta Crystallogr D Biol Crystallogr 57*, 1755-1762.
5. Emsley, P., and Cowtan, K. (2004) Coot: model-building tools for molecular graphics, *Acta Crystallogr D Biol Crystallogr 60*, 2126-2132.
6. Murshudov, G. N., Vagin, A. A., and Dodson, E. J. (1997) Refinement of macromolecular structures by the maximum-likelihood method, *Acta Crystallogr D Biol Crystallogr 53*, 240-255.
7. Painter, J., and Merritt, E. A. (2006) Optimal description of a protein structure in terms of multiple groups undergoing TLS motion, *Acta Crystallogr D Biol Crystallogr 62*, 439-450.
8. Kilz, S., Lenz, C., Fuchs, R., and Budzikiewicz, H. (1999) A fast screening method for the identification of siderophores from fluorescent Pseudomonas spp. by liquid chromatography/electrospray mass spectrometry, *J Mass Spectrom 34*, 281-290.